

1 **IgA autoantibodies target pulmonary surfactant in patients with severe COVID-19**

2

3 Tobias Sinnberg<sup>1,2\*</sup>, Christa Lichtensteiger<sup>3\*</sup>, Omar Hasan Ali<sup>3,4,5\*</sup>, Oltin T. Pop<sup>3</sup>, Mara Gilardi<sup>6</sup>,  
4 Lorenz Risch<sup>7,8,9</sup>, David Bomze<sup>3,10</sup>, Philipp Kohler<sup>11</sup>, Pietro Vernazza<sup>11</sup>, Werner C. Albrich<sup>11</sup>,  
5 Christian R. Kahlert<sup>11,12</sup>, Silvio D. Brugger<sup>13</sup>, Marie-Therese Abdou<sup>3</sup>, Carl Zinner<sup>6</sup>, Alexandar  
6 Tzankov<sup>6</sup>, Martin Röcken<sup>1,2,14</sup>, Lukas Kern<sup>15</sup>, Martin H. Brutsche<sup>15</sup>, Hubert Kalbacher<sup>16</sup>, Ana Velic<sup>17</sup>,  
7 Boris Maček<sup>17</sup>, Josef M. Penninger<sup>5,18</sup>, Matthias S. Matter<sup>6</sup> & Lukas Flatz<sup>1,3,5,19</sup>

8

9 \* T.S., C.L., and O.H.A. contributed equally.

10

11 Affiliations:

12 1. Department of Dermatology, University Hospital Tübingen, Liebermeisterstraße 25, 72076  
13 Tübingen, Germany

14 2. Cluster of Excellence iFIT (EXC 2180) Image Guided and Functionally Instructed Tumor  
15 Therapies, University Hospital Tübingen, Liebermeisterstraße 25, 72076 Tübingen, Germany

16 3. Institute of Immunobiology, Kantonsspital St. Gallen, Rorschacher Strasse 95, 9007 St. Gallen,  
17 Switzerland

18 4. Department of Medical Genetics, Life Sciences Institute, University of British Columbia, 2350  
19 Health Sciences Mall, Vancouver V6T 1Z3, Canada

20 5. Department of Dermatology, University Hospital Zurich, University of Zurich, Rämistrasse 100,  
21 8091 Zurich, Switzerland

22 6. Pathology, Institute of Medical Genetics and Pathology, University Hospital Basel, University of  
23 Basel, Schönbeinstrasse 40, 4031 Basel, Switzerland

24 7. Labormedizinisches Zentrum Dr. Risch, Wuhrstrasse 14, 9490 Vaduz, Liechtenstein

25 8. Center of Laboratory Medicine, University Institute of Clinical Chemistry, University Hospital  
26 Bern, University of Bern, INO-F, 3010 Bern, Switzerland

27 9. Faculty of Medical Sciences, Private University in the Principality of Liechtenstein, Dorfstrasse 24,  
28 9495 Triesen, Liechtenstein

- 1 10. Sackler Faculty of Medicine, Tel Aviv University, P.O. Box 39040, Tel Aviv 6997801, Israel
- 2 11. Division of Infectious Diseases and Hospital Epidemiology, Kantonsspital St. Gallen,
- 3 Rorschacher Strasse 95, 9007 St. Gallen, Switzerland
- 4 12. Department of Infectious Diseases and Hospital Epidemiology, Children's Hospital of Eastern
- 5 Switzerland, Claudiusstrasse 6, 9000 St. Gallen, Switzerland
- 6 13. Department of Infectious Diseases and Hospital Hygiene, University Hospital Zurich, University
- 7 of Zurich, Rämistrasse 100, 8091 Zurich, Switzerland
- 8 14. German Cancer Research Consortium (DKTK), German Cancer Research Center (DKFZ), Im
- 9 Neuenheimer Feld 280, 69120 Heidelberg, Germany
- 10 15. Lung Center, Kantonsspital St. Gallen, Rorschacher Strasse 95, 9007 St. Gallen, Switzerland
- 11 16. Institute of Clinical Anatomy and Cell Analysis, University of Tübingen, Österbergstraße 3,
- 12 72074 Tübingen, Germany
- 13 17. Proteome Center Tübingen, Interfaculty Institute for Cell Biology, University of Tübingen, Auf
- 14 der Morgenstelle 15, 72076 Tübingen, Germany
- 15 18. Institute of Molecular Biotechnology of the Austrian Academy of Sciences (IMBA),
- 16 Dr.-Bohr-Gasse 3, 1030 Vienna, Austria
- 17 19. Department of Dermatology, Venereology and Allergology, Kantonsspital St. Gallen,
- 18 Rorschacher Strasse 95, 9007 St. Gallen, Switzerland

19

20 Corresponding author:

21 Prof. Lukas Flatz, MD

22 Department of Dermatology, University Hospital Tübingen, Liebermeisterstraße 25, 72076 Tübingen,  
23 Germany; Phone: +49 7071 2984620; Email: [lukas.flatz@med.uni-tuebingen.de](mailto:lukas.flatz@med.uni-tuebingen.de)

24

1 **ABSTRACT**

2 Complications affecting the lung are hallmarks of severe coronavirus disease 2019 (COVID-19).  
3 While there is evidence for autoimmunity in severe COVID-19, the exact mechanisms remain  
4 unknown. Here, we established a prospective observational cohort to study lung specific  
5 autoantibodies (auto-Abs). Incubation of plasma from severe COVID-19 patients with healthy human  
6 lung tissue revealed the presence of IgA antibodies binding to surfactant-producing pneumocytes.  
7 Enzyme-linked immunosorbent assays (ELISA) and protein pull-downs using porcine surfactant  
8 confirmed the presence of auto-Abs binding to surfactant proteins in severe COVID-19 patients. Mass  
9 spectrometry and ELISAs with recombinant proteins identified IgA auto-Abs that target human  
10 surfactant proteins B and C. In line with these findings, lungs of deceased COVID-19 patients showed  
11 reduced pulmonary surfactant. Our data suggest that IgA-driven autoimmunity against surfactant may  
12 result in disease progression of COVID-19.

## 1 INTRODUCTION

2 The Coronavirus disease 2019 (COVID-19), caused by infection with severe acute respiratory  
3 syndrome coronavirus 2 (SARS-CoV-2), has rapidly evolved into a global pandemic with grave  
4 socio-economic implications that affects every country worldwide.<sup>1,2</sup> To date more than 100 million  
5 cases of infection with SARS-CoV-2 and over 2 million deaths have been reported across the globe.<sup>3</sup>  
6 While age and comorbidities have been established as predictors for clinical outcome,<sup>4</sup> there is a lack  
7 of validated factors that precede disease progression. Particular susceptibility factors, such as HLA  
8 haplotype,<sup>5</sup> blood type,<sup>6</sup> and genetic polymorphisms of SARS-CoV-2 target receptors including  
9 angiotensin converting enzyme 2 (ACE2)<sup>7</sup> have been proposed. Yet, they are not utilized in standard  
10 clinical management of COVID-19.<sup>8</sup>

11 Recent publications highlight a potential role of autoimmunity associated with COVID-19 severity, as  
12 many patients develop symptoms that resemble autoimmune diseases, such as antiphospholipid  
13 syndrome (APS), rheumatoid arthritis, and myositis.<sup>9-11</sup> Woodruff et al. have shown a surge of B-cell  
14 responses that resemble those found in systemic lupus erythematosus (SLE) and further revealed that  
15 high concentrations of neutralizing SARS-CoV-2 antibodies are associated with higher mortality.<sup>12</sup>  
16 Bastard et al. reported that autoantibodies (auto-Abs) against the type I-interferons interferons (IFN)  
17  $\alpha 2$  and IFN- $\omega$  inhibit the immune response against SARS-CoV-2, significantly increasing the  
18 likelihood of disease progression.<sup>13</sup> In line with these findings, an emerging report by Yang et al.  
19 demonstrates that severely ill patients develop various auto-Abs against immunomodulatory proteins  
20 that potentially perturb antiviral immune responses.<sup>14</sup> Additionally, several studies have shown  
21 significant elevations of APS-associated auto-Abs in severely ill patients, additionally explaining their  
22 observed hypercoagulability and vascular inflammation.<sup>11,15</sup> A further indication for the role of  
23 autoimmunity is the significant reduction of mortality in severe and critically ill COVID-19 patients  
24 by administration of dexamethasone,<sup>16</sup> and preventing deterioration of disease using tocilizumab.<sup>17</sup>  
25 Consequently, immunosuppression with dexamethasone has been widely established as standard  
26 treatment of severe illness<sup>18</sup> and other immunosuppressive drugs, such as colchicine and cyclosporine,  
27 show benefits in preliminary study data.<sup>19,20</sup>

1 While there is strong evidence for the role of autoimmunity in severe COVID-19, the exact  
2 mechanisms have not been elucidated. Kanduc et al. have demonstrated amino acid sequence  
3 similarities of the spike glycoprotein of SARS-CoV-2 and human surfactant-related proteins,  
4 suggesting a cross-reactivity of immune responses due to antigen mimicry.<sup>21</sup> Additional investigations  
5 reveal a higher rate of shared protein epitopes between SARS-CoV-2 and the human proteome than  
6 with other viruses, further supporting this finding.<sup>22,23</sup> In a recent paper, Zuniga et al. have shown IgG  
7 directed against annexin-2, a phospholipid-binding protein of the lung vasculature, is elevated in  
8 severe COVID-19, indicating antibody cross-reactivity.<sup>24</sup> While autoimmune antibodies with cross-  
9 reactivity have been proposed, a lung cell specific target has not yet been shown.

10 Here, we present that severe COVID-19 is significantly associated with an IgA-driven autoimmune  
11 response that targets surfactant proteins in type 2 pneumocytes. This may result in diminished  
12 surfactant and, thus, could drive progression of disease severity. We established a prospective  
13 observational study and collected plasma samples of COVID-19 patients with varying disease  
14 severity. Using immunofluorescence, we observed IgA bound to pulmonary surfactant in plasma of  
15 only severely ill COVID-19 patients. We then performed enzyme-linked immunosorbant assays  
16 (ELISAs) coated with poractant alfa, a natural surfactant extracted from porcine pulmonary tissue,  
17 which revealed significant binding of immunoglobulins (Ig). By mass spectrometry, we were able to  
18 identify surfactant proteins as candidate autoantigens. This was confirmed by ELISAs using  
19 recombinant human surfactant proteins. Lastly, immunofluorescence of lung tissue of deceased  
20 COVID-19 patients showed diminished surfactant. To summarize our findings, we identified IgA  
21 auto-Abs targeting surfactant proteins which demonstrate IgA-driven autoimmunity, likely  
22 contributing to compromised blood oxygenation. These data reveal an urgent need to explore the  
23 preservation of surfactant proteins by immunosuppression and surfactant replacement in patients with  
24 severe COVID-19.

25  
26  
27  
28

## 1 RESULTS

### 2 Damaged lung tissue in COVID-19 shows autoimmune gene expression signatures

3 Most COVID-19 patients with fatal outcome develop diffuse alveolar damage (DAD), a life-threatening  
4 destructive lung disease that leads to disturbed pulmonary function with reduced gas exchange.<sup>25</sup>  
5 Several pathologies, such as pulmonary edema, microthrombosis and fibrosis lead to respiratory  
6 failure of patients with DAD. DAD from COVID-19 patients (COVID-19 DAD) show less  
7 pronounced exudative changes and hemorrhages compared to non-COVID-19 DAD, as well as more  
8 microthromboses, pulmonary thromboembolisms and new vessel growth (intussusceptive  
9 angiogenesis), indicating additional drivers of pathology.<sup>25-27</sup> In addition, COVID-19 is characterized  
10 by an exaggerated immune response in the lung.<sup>28</sup> Thus, we hypothesized that the respiratory failure  
11 of COVID-19 patients may be further aggravated by auto-Abs against self-antigens evoked by an  
12 exaggerated immune activation. To understand if molecular pathways involved in autoimmunity are  
13 present in lung tissue of severe COVID-19 patients (n=11), we performed gene expression analysis  
14 with a panel specifically designed to analyze autoimmune disease (HTG EdgeSeq Immune Response  
15 Panel). As a control group, we used patients with a DAD (n=10) caused by other reasons such as  
16 drug-toxicity, lung surgery or myocardial infarction (**Fig. 1a; Supplementary Table 1**).  
17 Unsupervised hierarchical clustering by *k*-means revealed clear grouping of COVID-19 patients and  
18 non-COVID-19 patients in spite of both cohorts presenting with DAD (**Fig. 1b**). To explore, if  
19 networks of autoimmune diseases are activated in COVID-19 patients, we performed gene set  
20 enrichment analyses. To that end, we searched the Kyoto Encyclopedia of Genes and Genomes  
21 database (KEGG; <https://www.genome.jp/kegg/pathway.html>) for autoimmune diseases and selected  
22 “systemic lupus erythematosus (SLE)” and “autoimmune thyroid disease (ATD)”. To date, these  
23 autoimmune diseases are the only ones in KEGG that entail a substantial production of auto-Abs.  
24 While both pathways showed significant expression enrichment in lung tissue of COVID-19 autopsy  
25 samples (**Fig. 1c**), only the enrichment compared to SLE remained significant after false discovery  
26 rate (fdr)-adjustment (SLE normalized enrichment score: 1.6,  $P=0.0008$ , fdr-adjusted  $P=0.02$ ; vs.  
27 ATD normalized enrichment score: 1.9,  $P=0.01$ , fdr-adjusted  $P=0.10$ ). In conclusion, these data show  
28 that networks of autoimmune disorders with the production of auto-Abs are enriched in COVID-19

1 patients.

2

### 3 **Clinical study design**

4 In order to identify auto-Abs in patients with COVID-19 we enrolled N=46 individuals in a  
5 prospective monocentric observational study and collected plasma samples. The median age was 61  
6 years (interquartile range 55-70 years), and 32 (70%) were male. Patient characteristics are provided  
7 in **Supplementary Table 2**. Patients were divided into subgroups by COVID-19 severity based on  
8 clinical criteria.<sup>29</sup> In summary, we included 26 (57%) patients with critical, 13 (28%) with severe, and  
9 7 (15%) with asymptomatic illness. For simplicity, patients with critical and severe disease will be  
10 referred together as severe COVID-19. Additionally, we included plasma samples from healthy, non-  
11 infected patients for control measurements. Details on patient recruitment are provided in the Methods  
12 section.

13

### 14 **Autoimmune antibodies are elevated in severe COVID-19**

15 We assessed the presence of autoimmune-disease specific auto-Abs in COVID-19 patients and found  
16 several auto-Abs that were elevated in individuals suffering from severe COVID-19 compared to  
17 asymptomatic patients (**Fig. 1d**). Using the median antibody values of all cohorts, we calculated a  
18 cumulative autoimmunity score (CAS). As expected, the CAS in severe COVID-19 patients was  
19 significantly higher than in asymptomatic patients ( $P=0.02$ , two-tailed t-test, **Figure 1e**). In line with  
20 the literature,<sup>14</sup> our data showed elevated auto-Abs in severe COVID-19 compared to asymptomatic  
21 patients, suggesting a vigorous auto-Abs response associated with disease severity.

22

### 23 **Severe COVID-19 patients develop autoantibodies against proteins in type II pneumocytes**

24 Given that we have detected autoimmune gene expression signatures, as well as auto-Abs, we next  
25 determined the reactivity of auto-Abs in plasma samples from severe COVID-19 patients to any lung  
26 protein using indirect immunofluorescence. Here, we inoculated plasma of severe COVID-19 patients  
27 and healthy control patients with normal human alveolar lung tissue. We discovered specific binding  
28 of IgA antibodies to distinguished areas of lung tissue (**Fig. 2a**). IgG were discoverable to a lesser

1 extent (**Supplementary Fig. 1**). Given that type II pneumocytes are the primary pulmonary target of  
2 SARS-CoV-2,<sup>30</sup> we assessed mRNA expression from various lung alveolar cells using previously  
3 published data.<sup>31</sup> This revealed a characteristically high gene expression of surfactant proteins C  
4 (SFTPC), B (SFTPB), A1 and A2 in type II pneumocytes (**Fig. 2b**). To examine, whether COVID-19  
5 patients showed IgA and IgG derived autoreactivity against surfactant-producing cells, we performed  
6 immunofluorescence and co-stained for surfactant protein A as a surrogate marker for type II  
7 pneumocytes. This showed strong co-localization of IgA and surfactant (**Fig. 2c**), and, to a lesser  
8 extent, of IgG and surfactant (**Supplementary Fig. 2**). Thus, our data indicate that predominantly IgA  
9 auto-Abs bind to surfactant proteins in severe COVID-19 patients.

10

### 11 **IgA autoantibodies target surfactant protein B and C in patients with severe COVID-19**

12 In order to identify the target surfactant protein, we performed ELISA coated with poractant alfa.  
13 Poractant alfa is an extract of porcine lung surfactant that consists of various phospholipids and  
14 phospholipid-binding proteins, and is used as an intratracheal rescue therapy for infants with acute  
15 respiratory lung distress syndrome (ARDS).<sup>32</sup> ELISA results showed a significant presence of IgA  
16 ( $P=0.006$ , Mann-Whitney U test, **Fig. 3a**) and IgG ( $P=0.001$ , **Supplementary Fig. 3**) directed against  
17 poractant alfa in the plasma of severe COVID-19 patients compared to asymptomatic disease. Next,  
18 we identified protein components of poractant alfa using mass spectrometry, which confirmed the  
19 presence of SFTPB and SFTPC (**Fig. 3b**). To identify putative antigens, we prepared pull-down  
20 affinity columns: here we used pooled and immobilized Ig from severe COVID-19 patients ( $n=14$ )  
21 and uninfected healthy controls ( $n=5$ ), after their incubation with poractant alfa. The extract was  
22 analyzed by mass spectrometry to determine the Ig-captured proteins. Interestingly, SFTPB was the  
23 most abundant protein with high enrichment ( $\geq 10$ -fold) for captured proteins from plasma of severe  
24 COVID-19 patients (**Fig. 3c**). Next, we used recombinant proteins of SFTPB and SFTPC to determine  
25 the presence of autoreactive IgA and IgG in severe COVID-19 patients. The results showed a highly  
26 significant difference of IgA against SFTPB (severe vs. asymptomatic,  $P=0.001$ , Mann-Whitney U  
27 test) and for SFTPC (severe vs. asymptomatic,  $P=0.004$ ) (**Fig. 3d**). Conversely, they showed no  
28 significant difference for autoreactive IgG (**Supplementary Fig. 4**).



1

2 **Surfactant is diminished in lungs of deceased COVID-19 patients**

3 SARS-CoV-2 primarily infects cells via their angiotensin converting enzyme 2 (ACE2) receptors.<sup>33</sup>

4 By infecting alveolar type II epithelial cells, which are rich in ACE2 receptors on their surface,

5 SARS-CoV-2 directly influences the function and production of surfactant proteins.<sup>30</sup> Our data of

6 auto-Abs against surfactant protein suggest an additional mechanism of surfactant disturbance. To

7 investigate, whether surfactant in lung tissue of COVID-19 patients is affected, we assessed its

8 presence in deceased COVID-19 patients with DAD and compared it to patients with non-COVID-19

9 DAD, and healthy controls. As suggested by previously reported gene expression analysis,<sup>34</sup> the total

10 amount of surfactant was reduced in COVID-19 patients in comparison to non-COVID-DAD as well

11 as to healthy controls (**Fig. 3e**).

12 In summary, we identified novel IgA-driven autoimmune response against SFTPB and SFTPC in

13 severe COVID-19 patients, which is associated with diminished surfactant. Our data suggest that a

14 vigorous B-cell response against self-antigens can corrupt crucial components for alveolar gas

15 exchange, possibly explaining progression of COVID-19 to ARDS. We suggest further mechanistic

16 exploration of this hypothesis.

17

## 1    **METHODS**

### 2    **Gene expression analysis:**

3    Samples were included based on quality control criteria by the manufacturer (HTG Molecular  
4    Diagnostics, Tucson, AZ). These require that the percentage of overall reads allocated to the positive  
5    process control probe per sample is less than 28%, the read depth is at least 750000 and the relative  
6    standard deviation of reads allocated to each probe within a sample is greater than 0.094. In addition,  
7    only samples with a known postmortem interval were preserved for differential analysis. Differential  
8    expression analysis was conducted in R version 4.0.3 (R Project for Statistical Computing, Vienna,  
9    Austria) with the DESeq2 package using default settings. Count estimates were normalized with the  
10    median ratio method. Differential gene expressions for the contrast of COVID-19 patients with DAD  
11    vs. control patients with other DAD were modelled with a negative binomial distribution and  
12    subjected to a Wald significance test. Prior to heatmap visualization, the normalized counts were  
13    further  $\log_2$  transformed using a robust variance stabilization. The heatmap of genes with a  $|\log$   
14    fold change  $> 1$  was produced with the complexHeatmap package. Column sample clusters were  
15    obtained by k-means clustering with  $k = 2$  and row gene clusters by hierarchical clustering with  
16    complete linkage. Functional analysis was quantified via gene set enrichment. All genes in the  
17    autoimmune panel were pre-ranked using the Wald test statistic and submitted to the entire KEGG  
18    database of human pathways using the clusterProfiler package.

19

### 20    **Clinical study: patient recruitment, data and blood sample collection**

21    Patient data and blood collection was approved by the Ethics committee of Eastern Switzerland (study  
22    ID 2020-01006), and tissue collection by Ethics committee of Northern and Central Switzerland  
23    (study ID 2020-00969). The studies were performed in accordance with the Declaration of Helsinki  
24    guidelines.<sup>35</sup> Collection of patient data and samples (serum or plasma) was conducted from April 9,  
25    2020, to May 1, 2020 and tissue collection from March 13 2020 to May 4 2020. SARS-CoV-2  
26    infection of the severe COVID-19 cohort was confirmed by real-time reverse transcriptase-  
27    polymerase chain reaction<sup>36</sup> of nasopharyngeal swab samples. Infection of asymptomatic COVID-19  
28    was confirmed with serology of SARS-CoV-2 antibodies, using two independent antibody tests: SGIT

1 flex Covid 19, a lateral flow immunochromatographic assay (LFIA) (Sugentech, Daejeon, South  
2 Korea), and Elecsys Anti-SARS-CoV-2, an electro-chemiluminescence immunoassay (ECLIA)  
3 (Roche International Diagnostics AG, Rotkreuz, Switzerland). We defined a positive result as  
4 elevated SARS-CoV-2 IgG in the LFIA in the acute phase with confirmation by IgG in the ECLIA  
5 after 3-4 weeks. All blood samples of severe COVID-19 patients were obtained within the first two  
6 weeks of symptom onset. Due to the unknown primary infection of patients with asymptomatic  
7 COVID-19, blood draw at an unknown timepoint is assumed.

8

### 9 **Plasma isolation from whole blood**

10 Plasma samples were isolated from sodium-heparin whole blood (BD Vacutainer® CPT™ tubes,  
11 Becton Dickinson, NJ). Briefly, the tubes were centrifuged at room temperature (RT) at 1650 g for 20  
12 minutes at room temperature. The undiluted plasma was then aliquoted and stored at -80 °C for  
13 subsequent analysis.

14

### 15 **Antibody analysis**

16 Myositis and systemic sclerosis antibodies (i.e. Mi-2a, Mi-2b, TIF1g, MDA5, NXP2, SAE1, Ku, PM-  
17 SCL100, PM-SCL75, Jo-1, SRP, PL-7, PL-12, EJ, OJ, Ro5 for myositis; Scl-70, CENPA, CENPB,  
18 RP11 (RNAP-III), RP155 (RNAP-III), Fibrillarin, NOR-90, Th/To, PM-Scl100, PM-Scl75, Ku,  
19 PDGRF, Ro-52 for systemic sclerosis) were determined via immunoblot using the EuroBlotOne test  
20 system (Euroimmun AG, Lübeck, Germany), respectively, following the manufacturer's instructions.  
21 Autoantibodies against Cardiolipin,  $\beta$ -2-glycoprotein 1, double stranded DNA (dsDNA), cyclic  
22 citrullinated peptide (CCP), SSA1, SSA2, SSB, Sm, PR3, and MPO were determined by fluorescence  
23 enzyme immunoassay on a Unicap 250 analyzer (Thermo Fisher Scientific, Waltham, U.S.A.).  
24 Rheumatoid factor (RF) was determined by turbidimetry (COBAS 6000, Roche Diagnostics,  
25 Rotkreuz, Switzerland). Measurements were performed at the Labormedizinisches Zentrum Dr. Risch  
26 (Buchs, St. Gallen, Switzerland), an ISO 17025:2018 accredited medical laboratory. The cumulative  
27 autoimmunity score (CAE) for each patient was generated in two steps: First, we calculated the  
28 median value of all the analyses results of a given autoantibody. Second, we determined for each

1 patient, if the result is above (score of “1”) or below (score of “0”) that value. The CAE represents the  
2 sum of those scores across all autoantibodies for any given patient.

3

#### 4 **Indirect immunofluorescence**

5 Four serial frozen sections from 4 lung tissues from patients without COVID-19 infection were  
6 washed two times with PBS 0.1% Tween 20, for 5 min each. In a first step one section from each lung  
7 tissue was then incubated for 30 minutes at RT with plasma from severe COVID-19 patients (plasma  
8 pooled from three patients and diluted 1:3 in PBS), and another with serum from healthy donors  
9 (pooled from three individuals, diluted 1:3 in PBS), and two slides with PBS only (negative controls).  
10 After washing, one of the of the control slides was then incubated with sterile PBS for 30 min at room  
11 temperature, while the remaining three slides were incubated with anti-IgA FITC (Dako, catalog no.  
12 F0204; dilution 1:50) or anti-IgG FITC (Dako, catalog no. F0202; dilution 1:50) for 30 minutes at RT.  
13 Slides were then counterstained with DAPI (ThermoFisher, catalog no. D1306) and mounted using  
14 fluorescence mounting medium (Dako, catalog no. S3023). Slides were imaged and assessed using a  
15 Zeiss LSM 710 laser scanning microscope (Carl Zeiss AG, Oberkochen, Germany).

16

#### 17 **Co-localization immunofluorescence staining**

18 Fresh frozen lung tissues were incubated with the above described patients’ plasma pools diluted 1:3  
19 for 30 min RT. Immunofluorescence staining was performed as previously described.<sup>37-39</sup> Briefly,  
20 anti-surfactant (diluted 1:100 ab51891, Abcam), anti-IgA FITC and anti-IgG FITC primary antibodies  
21 (diluted 1:50, respectively F0316-F0202 Dako) were used. Then, the incubation with the serum  
22 secondary antibody alexa-fluor 647 (Invitrogen) was done. DAPI incubation for 10 minutes has been  
23 performed to stain the nuclei. Samples were mounted in prolong gold anti-fade mounting medium  
24 (Invitrogen) and scanned by confocal microscope (Ti2, Nikon, Tokyo, Japan). Images were analyzed  
25 using QuPath software<sup>40</sup> as previously reported.<sup>37</sup> Intensity fluorescence profile has been analyzed by  
26 Nikon software to determine the co-localization of the signals as previously reported.<sup>38</sup>

27

28

## 1 **SFTPB immunofluorescence staining**

2 We compared the presence of SFTPB in formalin-fixed paraffin-embedded lung tissues obtained from  
3 deceased patients with COVID-19 DAD, non-COVID-19 DAD and normal lungs as controls. Tissues  
4 were processed as previously described for immunofluorescence staining.<sup>37-39</sup> Briefly, antigen  
5 retrieval was performed, and tissues incubated with PBS 0.1% Tween-20. Staining using anti-SFTPB  
6 antibodies diluted 1:100 (NCL-SPPB) was done in blocking buffer for 1h at RT. Alexa-fluor 647  
7 (Invitrogen) was applied as secondary antibody. Controls for secondary antibody specificity were  
8 generated by substituting the primary antibody with blocking buffer only. All samples were incubated  
9 with DAPI for 10 minutes and mounted in prolong gold anti-fade mounting medium (Invitrogen) and  
10 scanned with the Ti2 confocal microscope (Nikon, Tokyo, Japan).

11

## 12 **Single cell RNA data analysis**

13 Single-cell RNA sequencing data of healthy lungs were obtained from the LungMap project<sup>31</sup> via the  
14 TopCell portal (<https://toppcell.cchmc.org/>). Counts were normalized to log2-transcripts per million  
15 (TPM) and compared across the 7 major epithelial cell types: type-1, and type-2 alveolar-, basal-,  
16 ciliated-, club-, and goblet cells, as well as ionocytes. Housekeeping genes were excluded from the  
17 analysis. Cell-specific genes were defined as those with overall expression  $\log_2\text{-TPM} > 5$  and at least  
18 4-fold higher expression in one or two particular cell types compared to all other cell types.

19

## 20 **Immunoglobulin isolation from COVID-19 plasma samples**

21 Plasma samples from 14 critical/severe COVID-19 patients and 5 asymptomatic patients were pooled  
22 and immunoglobulins were isolated from 1 ml each of the plasma pools using 4 mL protein L coupled  
23 agarose resin (Capto™ L, Cytiva Life Sciences, Amersham, UK) packed into 15 mL empty  
24 polypropylene columns (Chromabond, Machery-Nagel, Düren, Germany). After extensive washing  
25 with PBS-T (0.05% Tween 20) the immunoglobulins were eluted in 0.1 M glycine buffer pH 2.5. 50  
26 % of the isolated immunoglobulins from the pools were individually and chemically cross-linked onto  
27 1 g of CNBr-activated sepharose (CNBr-activated Sepharose® 4B, Cytiva) as recommended by the  
28 manufacturer and packed into 15 mL empty polypropylene columns (Chromabond, Machery-Nagel).

1 The protein content of 0.33 mL Curosurf® (poractant alfa, Chiesi Farmaceutici, Parma, Italy) was  
2 immuno-purified after acetone precipitation in 15 mL of PBS-T per column by overnight binding at  
3 4°C using a peristaltic pump (ISM597A, Ismatec, Wertheim, Germany) and a circuit flow rate of 0.5  
4 mL/min, washing with 100 ml of PBS-T and elution in glycine buffer pH 2.5.

5

#### 6 **Protein identification by mass spectrometry**

7 A SDS PAGE short gel purification was run with either acetone-precipitated 0.2 mL Curosurf® or the  
8 immuno-purified and eluted proteins and in-gel digestion with Trypsin was conducted as described  
9 previously.<sup>41</sup> Extracted peptides were desalted using C18 StageTips<sup>42</sup> and subjected to LC-MS/MS  
10 analysis. LC-MS/MS analyses were performed on an Easy-nLC 1200 UHPLC (Thermo Fisher  
11 Scientific, Waltham, MA) coupled to an QExactive HF Orbitrap mass spectrometer (Thermo Fisher  
12 Scientific) as described elsewhere,<sup>43</sup> or an Orbitrap Exploris 480 mass spectrometer (Thermo Fisher  
13 Scientific) as previously described.<sup>44</sup> Peptides were eluted with a 60 min segmented gradient at a flow  
14 rate of 200nl/min, selecting 20 most intensive peaks for fragmentation with HCD. The MS data was  
15 processed with MaxQuant software suite v.1.6.7.0<sup>45</sup> to measure the iBAQ which was used to calculate  
16 the relative protein level ( $riBAQ=iBAQ/(\Sigma iBAQ)$ ). Database search was provided against pig  
17 (121817 entries) and human (96817 entries) UniProt database using the Andromeda search engine.<sup>46</sup>

18

## 1 REFERENCES

- 2 1 Townsend, E. COVID-19 policies in the UK and consequences for mental health. *Lancet*  
3 *Psychiatry* **7**, 1014-1015, doi:10.1016/S2215-0366(20)30457-0 (2020).
- 4 2 Lane, H. C. & Fauci, A. S. Research in the Context of a Pandemic. *N Engl J Med*,  
5 doi:10.1056/NEJMe2024638 (2020).
- 6 3 John Hopkins University. *Coronavirus Resource Center*,  
7 <<https://coronavirus.jhu.edu/map.html>> (2020).
- 8 4 Wiersinga, W. J., Rhodes, A., Cheng, A. C., Peacock, S. J. & Prescott, H. C.  
9 Pathophysiology, Transmission, Diagnosis, and Treatment of Coronavirus Disease 2019  
10 (COVID-19): A Review. *JAMA* **324**, 782-793, doi:10.1001/jama.2020.12839 (2020).
- 11 5 Nguyen, A. *et al.* Human Leukocyte Antigen Susceptibility Map for Severe Acute  
12 Respiratory Syndrome Coronavirus 2. *J Virol* **94**, doi:10.1128/JVI.00510-20 (2020).
- 13 6 Severe Covid, G. G. *et al.* Genomewide Association Study of Severe Covid-19 with  
14 Respiratory Failure. *N Engl J Med* **383**, 1522-1534, doi:10.1056/NEJMoa2020283 (2020).
- 15 7 Hou, Y. *et al.* New insights into genetic susceptibility of COVID-19: an ACE2 and  
16 TMPRSS2 polymorphism analysis. *BMC Med* **18**, 216, doi:10.1186/s12916-020-01673-z  
17 (2020).
- 18 8 World Health Organization (WHO). *Clinical management of COVID-19, 27 May 2020*,  
19 <<https://apps.who.int/iris/rest/bitstreams/1278777/retrieve>> (2020).
- 20 9 Malas, M. B. *et al.* Thromboembolism risk of COVID-19 is high and associated with a higher  
21 risk of mortality: A systematic review and meta-analysis. *EClinicalMedicine* **29**, 100639,  
22 doi:10.1016/j.eclinm.2020.100639 (2020).
- 23 10 Vlachoyiannopoulos, P. G. *et al.* Autoantibodies related to systemic autoimmune rheumatic  
24 diseases in severely ill patients with COVID-19. *Ann Rheum Dis* **79**, 1661-1663,  
25 doi:10.1136/annrheumdis-2020-218009 (2020).
- 26 11 Hasan Ali, O. *et al.* Severe COVID-19 is associated with elevated serum IgA and  
27 antiphospholipid IgA-antibodies. *Clin Infect Dis*, doi:10.1093/cid/ciaa1496 (2020).

- 1 12 Woodruff, M. C. *et al.* Extrafollicular B cell responses correlate with neutralizing antibodies  
2 and morbidity in COVID-19. *Nat Immunol* **21**, 1506-1516, doi:10.1038/s41590-020-00814-z  
3 (2020).
- 4 13 Bastard, P. *et al.* Autoantibodies against type I IFNs in patients with life-threatening COVID-  
5 19. *Science* **370**, doi:10.1126/science.abd4585 (2020).
- 6 14 Wang, E. Y. *et al.* Diverse Functional Autoantibodies in Patients with COVID-19. Preprint at  
7 <https://www.medrxiv.org/content/10.1101/2020.12.10.20247205v5> (2020).
- 8 15 Zuo, Y. *et al.* Prothrombotic autoantibodies in serum from patients hospitalized with COVID-  
9 19. *Sci Transl Med* **12**, doi:10.1126/scitranslmed.abd3876 (2020).
- 10 16 Horby, P. *et al.* Dexamethasone in Hospitalized Patients with Covid-19 - Preliminary Report.  
11 *N Engl J Med*, doi:10.1056/NEJMoa2021436 (2020).
- 12 17 Salama, C. *et al.* Tocilizumab in Patients Hospitalized with Covid-19 Pneumonia. *N Engl J*  
13 *Med* **384**, 20-30, doi:10.1056/NEJMoa2030340 (2021).
- 14 18 US Center for Disease Control (CDC). *COVID-19 treatment guidelines*,  
15 <<https://www.covid19treatmentguidelines.nih.gov/therapeutic-management>> (2020).
- 16 19 Lopes, M. I. F. *et al.* Beneficial effects of colchicine for moderate to severe COVID-19: an  
17 interim analysis of a randomized, double-blinded, placebo controlled clinical trial. Preprint at  
18 <https://www.medrxiv.org/content/10.1101/2020.08.06.20169573v2> (2020).
- 19 20 Guisado-Vasco, P. *et al.* Clinical characteristics and outcomes among hospitalized adults with  
20 severe COVID-19 admitted to a tertiary medical center and receiving antiviral, antimalarials,  
21 glucocorticoids, or immunomodulation with tocilizumab or cyclosporine: A retrospective  
22 observational study (COQUIMA cohort). *EClinicalMedicine* **28**, 100591,  
23 doi:10.1016/j.eclinm.2020.100591 (2020).
- 24 21 Kanduc, D. & Shoenfeld, Y. On the molecular determinants of the SARS-CoV-2 attack. *Clin*  
25 *Immunol* **215**, 108426, doi:10.1016/j.clim.2020.108426 (2020).
- 26 22 Kanduc, D. From Anti-SARS-CoV-2 Immune Responses to COVID-19 via Molecular  
27 Mimicry. *Antibodies (Basel)* **9**, doi:10.3390/antib9030033 (2020).



- 1 23 Kanduc, D. & Shoenfeld, Y. Molecular mimicry between SARS-CoV-2 spike glycoprotein  
2 and mammalian proteomes: implications for the vaccine. *Immunol Res* **68**, 310-313,  
3 doi:10.1007/s12026-020-09152-6 (2020).
- 4 24 Zuniga, M. *et al.* Autoimmunity to the Lung Protective Phospholipid-Binding Protein  
5 Annexin A2 Predicts Mortality Among Hospitalized COVID-19 Patients. Preprint at  
6 <https://www.medrxiv.org/content/10.1101/2020.12.28.20248807v1> (2021).
- 7 25 Menter, T. *et al.* Postmortem examination of COVID-19 patients reveals diffuse alveolar  
8 damage with severe capillary congestion and variegated findings in lungs and other organs  
9 suggesting vascular dysfunction. *Histopathology* **77**, 198-209, doi:10.1111/his.14134 (2020).
- 10 26 Ackermann, M. *et al.* Pulmonary Vascular Endothelialitis, Thrombosis, and Angiogenesis in  
11 Covid-19. *N Engl J Med* **383**, 120-128, doi:10.1056/NEJMoa2015432 (2020).
- 12 27 Borczuk, A. C. *et al.* COVID-19 pulmonary pathology: a multi-institutional autopsy cohort  
13 from Italy and New York City. *Mod Pathol* **33**, 2156-2168, doi:10.1038/s41379-020-00661-1  
14 (2020).
- 15 28 Nienhold, R. *et al.* Two distinct immunopathological profiles in autopsy lungs of COVID-19.  
16 *Nat Commun* **11**, 5086, doi:10.1038/s41467-020-18854-2 (2020).
- 17 29 Gandhi, R. T., Lynch, J. B. & Del Rio, C. Mild or Moderate Covid-19. *N Engl J Med* **383**,  
18 1757-1766, doi:10.1056/NEJMcp2009249 (2020).
- 19 30 Hu, B., Guo, H., Zhou, P. & Shi, Z. L. Characteristics of SARS-CoV-2 and COVID-19. *Nat*  
20 *Rev Microbiol*, doi:10.1038/s41579-020-00459-7 (2020).
- 21 31 Vieira Braga, F. A. *et al.* A cellular census of human lungs identifies novel cell states in  
22 health and in asthma. *Nat Med* **25**, 1153-1163, doi:10.1038/s41591-019-0468-5 (2019).
- 23 32 US Food and Drug Administration (FDA). *CUROSURF (poractant alfa) intratracheal*  
24 *suspension*,  
25 <[https://www.accessdata.fda.gov/drugsatfda\\_docs/label/2014/020744s0281bl.pdf](https://www.accessdata.fda.gov/drugsatfda_docs/label/2014/020744s0281bl.pdf)> (2020).
- 26 33 Monteil, V. *et al.* Inhibition of SARS-CoV-2 Infections in Engineered Human Tissues Using  
27 Clinical-Grade Soluble Human ACE2. *Cell* **181**, 905-913 e907,  
28 doi:10.1016/j.cell.2020.04.004 (2020).

- 1 34 Islam, A. & Khan, M. A. Lung transcriptome of a COVID-19 patient and systems biology  
2 predictions suggest impaired surfactant production which may be druggable by surfactant  
3 therapy. *Sci Rep* **10**, 19395, doi:10.1038/s41598-020-76404-8 (2020).
- 4 35 World Medical Association. *Declaration of Helsinki – Ethical Principles for Medical  
5 Research Involving Human Subjects*, <[https://www.wma.net/policies-post/wma-declaration-  
6 of-helsinki-ethical-principles-for-medical-research-involving-human-subjects/](https://www.wma.net/policies-post/wma-declaration-of-helsinki-ethical-principles-for-medical-research-involving-human-subjects/)> (2020).
- 7 36 Corman, V. M. *et al.* Detection of 2019 novel coronavirus (2019-nCoV) by real-time RT-  
8 PCR. *Euro Surveill* **25**, doi:10.2807/1560-7917.ES.2020.25.3.2000045 (2020).
- 9 37 Gilardi, M. *et al.* Tipifarnib as a Precision Therapy for HRAS-Mutant Head and Neck  
10 Squamous Cell Carcinomas. *Mol Cancer Ther* **19**, 1784-1796, doi:10.1158/1535-7163.MCT-  
11 19-0958 (2020).
- 12 38 Banerjee, S. *et al.* Anti-KIT DNA Aptamer for Targeted Labeling of Gastrointestinal Stromal  
13 Tumor. *Mol Cancer Ther* **19**, 1173-1182, doi:10.1158/1535-7163.MCT-19-0959 (2020).
- 14 39 Wang, Z. *et al.* Syngeneic animal models of tobacco-associated oral cancer reveal the activity  
15 of in situ anti-CTLA-4. *Nat Commun* **10**, 5546, doi:10.1038/s41467-019-13471-0 (2019).
- 16 40 Bankhead, P. *et al.* QuPath: Open source software for digital pathology image analysis. *Sci  
17 Rep* **7**, 16878, doi:10.1038/s41598-017-17204-5 (2017).
- 18 41 Borchert, N. *et al.* Proteogenomics of *Pristionchus pacificus* reveals distinct proteome  
19 structure of nematode models. *Genome Res* **20**, 837-846, doi:10.1101/gr.103119.109 (2010).
- 20 42 Rappsilber, J., Mann, M. & Ishihama, Y. Protocol for micro-purification, enrichment, pre-  
21 fractionation and storage of peptides for proteomics using StageTips. *Nat Protoc* **2**, 1896-  
22 1906, doi:10.1038/nprot.2007.261 (2007).
- 23 43 Schmitt, M. *et al.* Quantitative Proteomics Links the Intermediate Filament Nestin to  
24 Resistance to Targeted BRAF Inhibition in Melanoma Cells. *Mol Cell Proteomics* **18**, 1096-  
25 1109, doi:10.1074/mcp.RA119.001302 (2019).
- 26 44 Theurillat, I. *et al.* Extensive SUMO Modification of Repressive Chromatin Factors  
27 Distinguishes Pluripotent from Somatic Cells. *Cell Rep* **32**, 108146,  
28 doi:10.1016/j.celrep.2020.108146 (2020).

- 1 45 Cox, J. & Mann, M. MaxQuant enables high peptide identification rates, individualized  
2 p.p.b.-range mass accuracies and proteome-wide protein quantification. *Nat Biotechnol* **26**,  
3 1367-1372, doi:10.1038/nbt.1511 (2008).
- 4 46 Cox, J. *et al.* Andromeda: a peptide search engine integrated into the MaxQuant environment.  
5 *J Proteome Res* **10**, 1794-1805, doi:10.1021/pr101065j (2011).
- 6

1    **ACKNOWLEDGEMENTS**

2    We thank Dorothea Hillmann (Labormedizinisches Zentrum Dr. Risch) for her contributions to  
3    laboratory analyses.

4

5    **Funding:** This research was supported by grants from the Swiss National Science Foundation  
6    (PP00P3\_157448 to L.F., P400PM\_194473 to O.H.A., and 320030\_189275 to M.S.M.), the Research  
7    Fund of the Kantonsspital St. Gallen (20/20 to L.F.), the Promedica Foundation (1449/M to S.D.B.),  
8    and the Botnar Research Centre for Child Health Emergency Response to COVID-19 Grant (to C.Z.,  
9    M.S.M., and A.T.).

10

11    **Competing interests:** J.M.P. is founder and shareholder of Apeiron (Vienna, Austria), developing  
12    soluble ACE2 as a COVID-19 therapy. J.M.P. has no direct competing interest relating to the paper or  
13    data presented in the paper. M.S.M. has received speaker honoraria from Thermo Fisher Scientific  
14    (Waltham, MA) and honoraria as an advisory board member from Novartis AG (Basel, Switzerland).  
15    All other authors have no competing interests to declare.

16

17    **Supplementary information** is available for this paper.

18

1 **FIGURE LEGENDS**

2 **Fig. 1: a**, Representative images of diffuse alveolar disease (DAD) from COVID-19 patients and non-  
3 COVID-19 patients show hyaline membrane formation, desquamation and beginning of septal  
4 fibrosis. Hematoxylin and eosin staining. **b**, RNA sequencing data of DAD resulting from COVID-19  
5 (n=11) and other causes (n=10) reveals a clustered upregulation of genes. **c**, Gene set enrichment  
6 analysis shows a significant correlation of the systemic lupus erythematosus enrichment pattern and  
7 COVID-19 ( $P=0.02$ ). A trend can be observed for autoimmune thyroid disease. **d**, Heatmap (center  
8 panel) displaying fold-levels of autoantibodies (auto-Abs) relative to the upper reference limits of the  
9 diagnostic laboratory assays, in descending order (left to right). The left panel shows autoimmune  
10 diseases, while the right panel lists associated auto-Abs. The bottom panel indicates the individual  
11 patients, with severe (marine blue, n=39) or asymptomatic (light blue, n=7) COVID-19.  
12 Abbreviations: APS = antiphospholipid syndrome, RA = rheumatoid arthritis, SLE = systemic lupus  
13 erythematosus, Vasc = vasculitis. **e**, Comparison of the cumulative autoimmunity scores derived from  
14 the median value of each antibody. Patients with severe COVID-19 score (n=39) significantly higher  
15 than asymptomatic patients (n=7,  $P=0.02$ ). Score calculation is described in the Methods section.

16  
17 **Fig. 2: a**, Indirect Immunofluorescence of lung tissue shows that IgA antibodies are present in diffuse  
18 alveolar damage of COVID-19 patients. **b**, RNA-seq expression of type II pneumocytes, the main  
19 producer of surfactant, shows abundant overexpression of surface proteins C (SFTPC), B (SFTPB),  
20 A1 (SFTPA1) and A2 (SFTPA2). **c**, Immunofluorescence staining of lung tissue with serum from  
21 severely ill COVID-19 patients shows co-localization of IgA binding with surfactant. Co-localization  
22 of IgA and the target protein is visualized in the right lower graph.

23  
24 **Fig. 3: a**, ELISA with poractant alfa (Curosurf®) demonstrates that significantly more IgA is binding  
25 in plasma from severe COVID-19 (n=18) compared to asymptomatic patients (n=6; mean with 95%  
26 CI,  $P=0.006$ ). **b**, Mass spectrometry of poractant alfa lists abundance of surfactant binding proteins B  
27 (SFTPB) and C (SFTPC). **c**, Pull-downs of poractant alfa reveal immunoglobulins binding to SFTPB  
28 predominantly in severe COVID-19 samples. **d**, ELISA with recombinant proteins show that patients

1 with severe COVID-19 (n=18) have significantly more IgA against SFTPB ( $P=0.001$ ) and  
2 significantly more IgA against SFTPC ( $P=0.004$ ) than asymptomatic patients (n=6) in the blood  
3 (mean with 95% CI). **e**, Indirect immunofluorescence with healthy lung tissue indicates reduced  
4 amounts of surfactant in non-COVID-19 diffuse alveolar damage (DAD) than in COVID-19 DAD.  
5

**Fig.1:** COVID-19 patients with severe illness have a distinct mRNA expression pattern in damaged alveolar tissue and elevated autoantibodies in their blood.

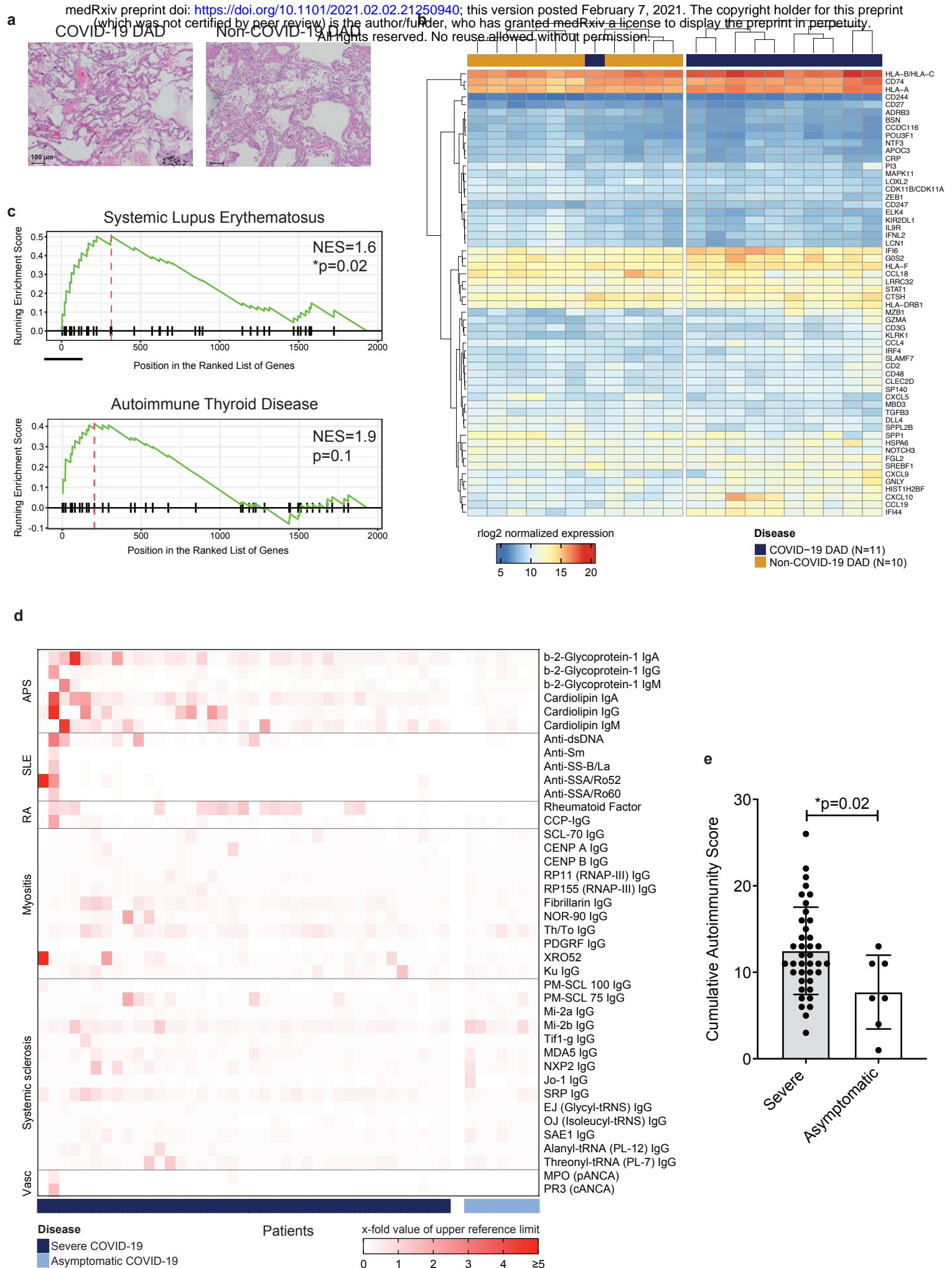


**Fig. 2: Immunoglobulins of severe COVID-19 patients co-localize with surfactant in lung tissue.**

medRxiv preprint doi: <https://doi.org/10.1101/2021.04.25.250940>; this version posted February 17, 2021. The copyright holder for this preprint (which was not certified by peer review) is the author/funder, who has granted medRxiv a license to display the preprint in perpetuity.

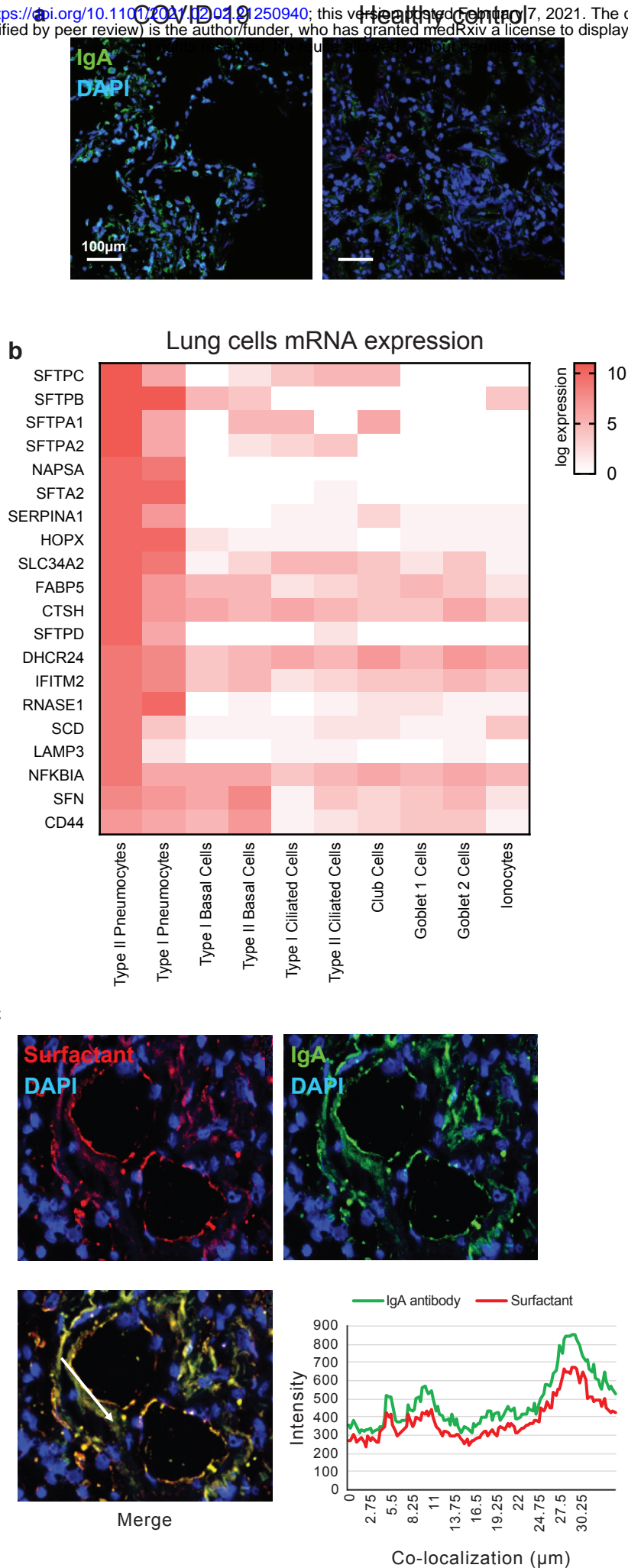




**Fig. 3: Severe COVID-19 is associated with elevated IgA against surfactant proteins B and C, and shows diminished alveolar surfactant.**

medRxiv preprint doi: <https://doi.org/10.1101/2021.02.02.21250940>; this version posted February 7, 2021. The copyright holder for this preprint (which was not certified by peer review) is the author/funder, who has granted medRxiv a license to display the preprint in perpetuity. All rights reserved. No reuse allowed without permission.

